Desalination and Water Treatment
www.deswater.com
doi: 10.5004/dwt.2023.29953

313 (2023) 49–56
November

Development of a ceramic membrane on a flat support for the treatment of an industrial effluent

Oumema Jlassi[a], Sofian Louhichi[b], Sabeur Khemakhem[a,*]

[a]*Laboratoire des Sciences de Matériaux et Environnement, Faculté des Sciences de Sfax, Université de Sfax, Route de Soukra Km 4, 3038 Sfax, Tunisia, emails: Khemakhem_sabeur@yahoo.fr (S. Khemakhem), jlassiomema863@gmail.com (O. Jlassi)*
[b]*Direction de la Recherche Scientifique-Gabés, Groupe Chimique Tunisie, email: louhichi_sofien@yahoo.fr*

Received 15 March 2023; Accepted 4 September 2023

ABSTRACT

The central focus of this research work is upon the development and characterization of a new ceramic microfiltration membrane. The support was prepared in a flat configuration using 100 μm calibrated powder made from mixed natural clay and natural phosphate. The firing temperature of the support amounts to 1,050°C for 3 h. After firing, the produced support was characterized using multiple methods (infrared spectroscopy, permeability, mechanical strength, scanning electronic microscopy, and mercury porosimeter). This support has subsequently become ready to prepare the microfiltration layer based on titanium oxide (TiO_2) through the use of the slip-casting method. The MF layer was firing to 950°C for consolidation. This microfiltration membrane has a permeability of 1,566.9 L/h·m²·bar. Finally, the membrane application to the treatment of textile effluents by photocatalysis revealed a good degradation of dyes with a removal rate of 97.41%.

Keywords: Microfiltration membrane; Flat configuration; Slip-casting method; Treatment of textile effluents; Photocatalysis

1. Introduction

Notably, ceramic membranes were synthesized through investing in an inorganic material such as titanium [1,2], alumina [3], silicon carbide [4,5], zirconium oxides [6,7], or some glassy materials [8,9]. Basically, ceramic membranes exhibit a sandwich-like structure of three layers [10,11]. The first layer corresponds to the support layer, the second or middle layer stands for the transition layer, and the last refers to the function layer. As its name suggests, the support layer is beneficial in terms of providing support and mechanical strength to the membrane system. The transition layer is significant in terms of preventing particles from moving through the membrane [10]. The function layer represents a crucial part of the system, serving to identify the membrane [12]. Relying on this layer, the membrane system is divided into multiple categories like microfiltration, ultrafiltration, and nanofiltration.

Inorganic ceramic membranes display certain merits over polymeric membranes, involving high mechanical thermal, strength, and chemical stability [10,11]. The membranes can withstand a very wide variety of temperatures and pH conditions owing to their thermally and chemically inert ceramic character. Additionally, they do not present irreversible structural changes that may influence their operational behavior. Microporous glasses, zeolites [13,14], titania, γ-alumina [15], and zirconia are frequently invested in the elaboration of ceramic membrane materials. The methods applied to prepare the inorganic ceramic membrane include mostly the following methods: chemical extraction, sol–gel method [16], solid-state sintering, phase-separation, chemical vapor deposition [17], and synthesis. However, inorganic ceramic membranes exhibit a wide distribution of pore sizes that are relatively large (≥600 nm), making them ineffective in separation processes including microfiltration, UF, and NF.

* Corresponding author.

Currently, using membrane separation processes is becoming highly significant in numerous industrial applications. This refers basically to their high effectiveness in terms of such separation processes as wastewater treatment in industrial effluents, food industries, and additional environmental applications [18].

In this respect, ceramic membranes display high chemical and thermal stability, long life, pressure resistance, and good mechanical strength with regard to organic membranes [19,20]. These inorganic membranes are notably made of alumina, silica, zircon and titanium [21,22] clay [23], kaolin [24], and phosphate [25].

While preparing the ceramic membrane, local clays were invested in order to elaborate flat and tubular ceramic membranes for the microfiltration process. Multiple researchers have addressed the development of low-cost ceramic membranes for microfiltration relying on natural materials. Some scientists have produced and characterized flat and tubular ceramic microfiltration membranes resting on natural Moroccan pozzolan [26,27]. Others have developed new tubular ceramic membranes derived from local Moroccan perlite so as to treat industrial wastewater [28]. Their work has interestingly highlighted outstanding separation properties.

Membrane selectivity is accomplished through the deposition of a porous thin layer of inorganic oxides like ZrO_2 and TiO_2 [29,30]. In order to guarantee the separation of solutes through suitable a pore radius, the deposition process needs to be selected carefully. Meanwhile, the support grants mechanical strength [31,32]. It is therefore noteworthy to observe that ceramic membranes display an asymmetric and composite structure formed by the deposition of a layer on previously fabricated support; such deposition can be achieved by slip-casting [33]; dip coating [34], and sol–gel [35]. The prepared membranes presented promising separation characteristics when implemented in various industrial wastewaters [36].

Within this framework, this research paper focuses on the development and characterization of microfiltration membranes generated by the slip-casting method on a flat ceramic support based on TiO_2. The prepared membranes were invested in to treat textile effluents through photocatalysis.

2. Characterization of the powder

2.1. Raw materials

As far as our study is concerned, the raw materials serving to prepare the ceramic support were: Tunisian natural phosphate and clay, both derived from the SEKHIRA region. The used phosphate presents a high organic matter content, enabling us to create pores without synthetic additives.

2.2. IR spectrum

IR spectroscopy is among the used methods to identify the groups that characterize the functions. The powder tested using IR spectral analysis is depicted in Fig. 1. An IR transmittance spectrum of the ground sample was determined in the 4,000–400 cm^{-1} range with a "Perkin Elmer" spectrophotometer. The IR spectrum of our sample exhibits a band of 3,625 cm^{-1} assigned to the characteristics of the stretching of structural hydroxyl groups OH [37], A characteristic band is recorded at 1,637.5 cm^{-1} corresponding to the OH deformation of water [37]. The peaks around 1,427 and 875 cm^{-1} are assigned to the presence of $CaCO_3$ [38]. The adsorption band around 1,004 cm^{-1} is suggestive of the antisymmetric elongation of Si–O [39]. The band located at 802 cm^{-1} is ascribed to the vibration of the stretching of Si–O–Si [40]. The characteristic band recorded at 468 cm^{-1} is attributed to the valence vibration of the Si–O group [41].

2.3. Thermal analysis

Thermogravimetric analysis (TGA) was conducted so as to specify the mass loss due to an increase in temperature. The temperature rise program is 10°C/min up to 1,050°C. Fig. 2 illustrates a first loss in mass of 3.31% between 350 and 400 K, which stands for the condensation of water resulting from the elimination of the hydroxyl groups

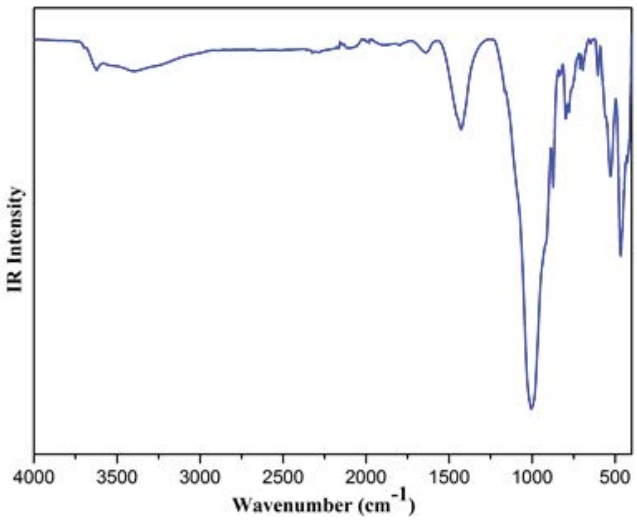

Fig. 1. IR spectrum of 50% clay and 50% phosphate.

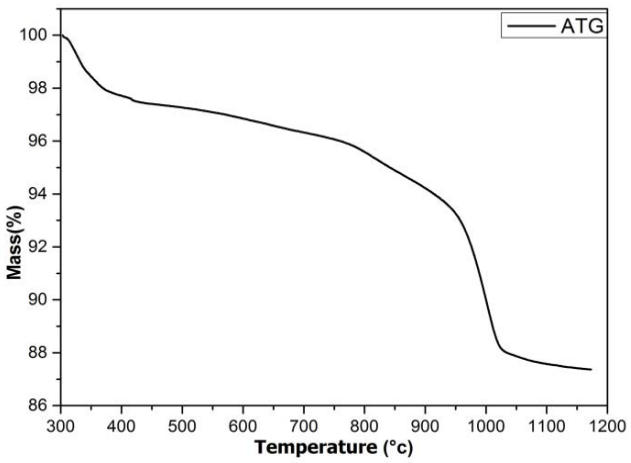

Fig. 2. Thermogravimetric analysis curve.

on the surface [42]. A second loss in mass of 3% between 700 and 900 K accounts for the thermal decomposition of mineral carbonates [43]. A third loss in mass of 4.11% occurred between 1,000 and 1,100 K, indicating sintering.

3. Elaboration and characterization of support

3.1. Elaboration of porous support

The dried homogeneous mixture of 50% phosphate and 50% clay (<150 μm) was compacted uniaxially twice: a first pressing followed by a second one with a pressing time that does not exceed 4 s, under 120 MPa in cylindrical molds creating flat discs, were next sintered in a programmable oven. This double pressing step is necessary as it helps ensure a more uniform thickness across the membrane. This uniformity is significant for consistent membrane performance. It can equally increase the density of the membrane material in order to improve its mechanical strength and make it more robust and less susceptible to damage during use. The thermal cycling was performed in four steps:

A first annealing of 2 h at 250°C with a rate of rise of 2°C/min to ensure the evaporation of the residual water, a second annealing of 2 h at 450°C with a rise rate of 2°C/min to degrade the organic matter present in the phosphate, a third annealing of 2 h 30 min for dehydration and a fourth annealing at the sintering temperature of 1,050°C, with a rise rate of 2°C/min.

3.2. IR spectrum

The IR spectrum of the sintered sample at 1,050°C (Fig. 3) reveals that the 1,979 cm^{-1} band is ascribed to the characteristics of the stretching of CO [44], which corroborates the presence of carbonates and other organic impurities in the clay. The peaks at 1,028 and 959 cm^{-1} are assigned to the antisymmetric elongation vibration of the PO_4 groupings [45]. Peaks 599 and 566 cm^{-1} refer to the antisymmetric deformation of the PO_4 group [46]. The band towards 457 cm^{-1} corresponds to the valence vibration of the Si–O group [41].

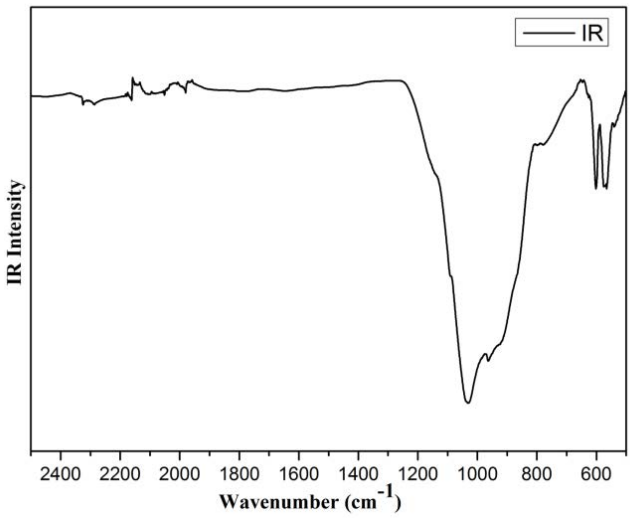

Fig. 3. IR spectrum of 50% clay and 50% phosphate sintered at 1,050°C.

3.3. Mechanical resistance

The three-point bending method was applied in order to determine the mechanical strength of the ceramic support cooked at 1,050°C. Departing from this test, it can be inferred based on Fig. 4 that the breaking stress (σ) is maximum at the sintering temperature (σ = 27.26 MPa). It seems therefore, that this is the most adequate temperature to ensure convenient mechanical strength.

3.4. Determination of support permeability

The pure water permeability of the support was tested on a laboratory-scale filtration pilot (Fig. 5). This permeability of the support was specified through the flow values estimated after stabilization. The flow of water permeation basically evolves as a function of time as stabilizes. Its value depends largely upon the pressure fixed with reference to the Darcy law. The flow increases along a linear line when the pressure increases. The permeability of the support (Fig. 6) is of the order of 2,526 ($L/h{\cdot}m^2{\cdot}bar$).

3.5. SEM image and EDX analysis

EDX analysis of the surface of the membrane demonstrates a high amount of Si with O, Ca, Al, etc. A similar microstructure of SEM images was obtained from a layer coated on porous clay-phosphate supports. It was detected that the layer was homogeneous, without cracks and firmly adhered to porous clay-phosphate material. The transversal view of the SEM image (Fig. 7a) and the linear EDX analysis of the image (Fig. 7b) exhibited a regular membrane thickness of 100 μm, while Ca and Si corresponded to the abandoned elements.

3.6. Mercury porosimetry

The mercury porosimeter allowed us to determine the distribution of pore diameters as well as the open porous volume of a ceramic support relying on clay and sintered phosphate at 1,050°C (Fig. 8). The differential intrusion

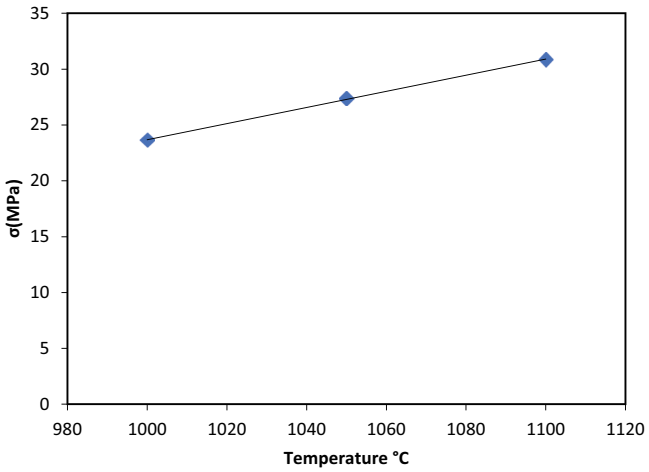

Fig. 4. Evolution of the stress at break (σ) of the substrate as a function of the sintering temperature.

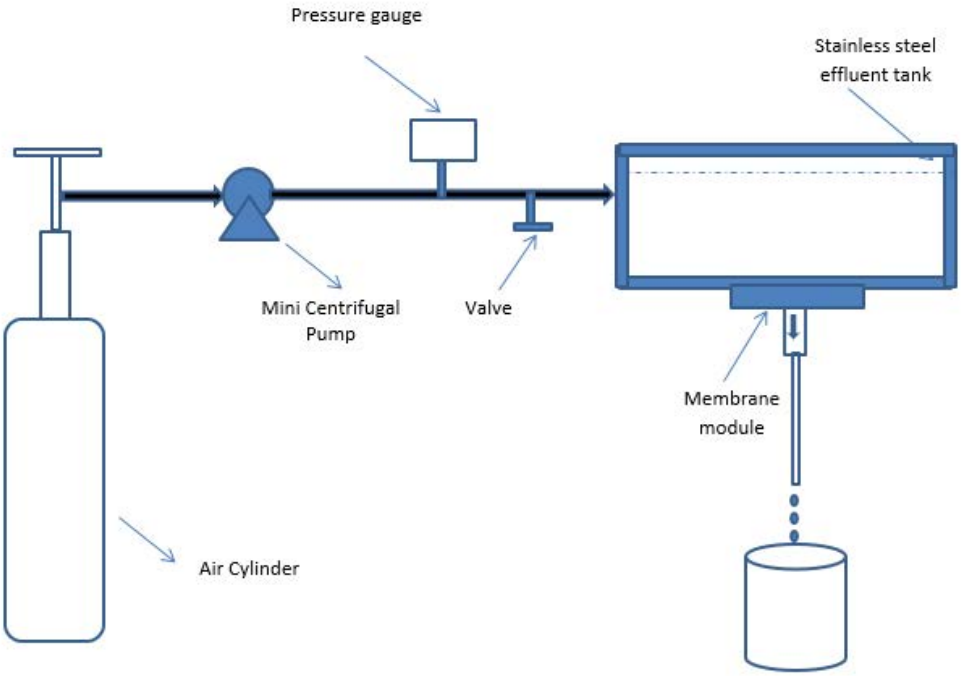

Fig. 5. Laboratory pilot.

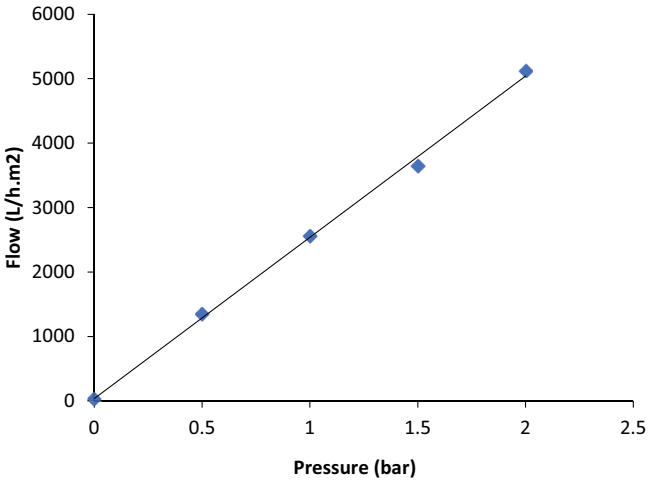

Fig. 6. Evolution of the flow (L/h·m^2) of the support according to the pressure (bar).

curve as a function of the diameter of the pores plotted in Fig. 8 reveals that the served supports at the optimal sintering temperature of 1,050°C have an average pores diameter of 10.36 μm with an average porosity of 41.66%.

4. Elaboration and characterization of the microfiltration layer

In order to develop the microfiltration layer, titanium oxide (TiO_2) was invested as a powder. Hence, by means of the dip-coating method, TiO_2 powder and distilled water were mixed with organic binder (12% solution by mass of PVA) respecting the following percentages: 5%, 65%, and 30%. The deposition time amounted to about 5 min. Following drying at room temperature for 24 h, the microfiltration layer was sintered at 950°C for 2 h.

The sintering program consists of a first 1 h level at 300°C corresponding to the departure of water and APV and a second level of 2 h at 950°C. These temperatures should not interfere with sintering to avoid the risk of cracking membranes.

The deposition of a microfiltration layer on the ceramic support is an intrinsic step in the manufacture of membranes. One of the main reasons for the deposition of this layer is to improve the separation efficiency as well as the selectivity of the membrane and to reduce the pore diameter with smaller pore sizes, which will be implemented by the process dip-coating method [38]. The active layer is designed to have specific characteristics that allow it to selectively retain or separate certain components of a mixture. In the case of ultrafiltration membranes, the layer is designed to efficiently remove particles and macromolecules while allowing small molecules and solvents to move through.

As for the permeability test, the ceramic membrane was applied to a filtration device. The chosen flat ceramic membrane was conditioned in pure water for 24 h before the filtration tests were conducted. The average permeability of the titanium oxide microfiltration membrane depicted in Fig. 9 amounted to 1566.9 L/h·m^2·bar.

5. Application of the membrane to the treatment of the dye (turquoise blue) by photocatalysis

To ensure the degradation of the turquoise blue under the presence of the light ray, the phenomenon of photocatalysis using the TiO_2 as a photocatalyst was selected.

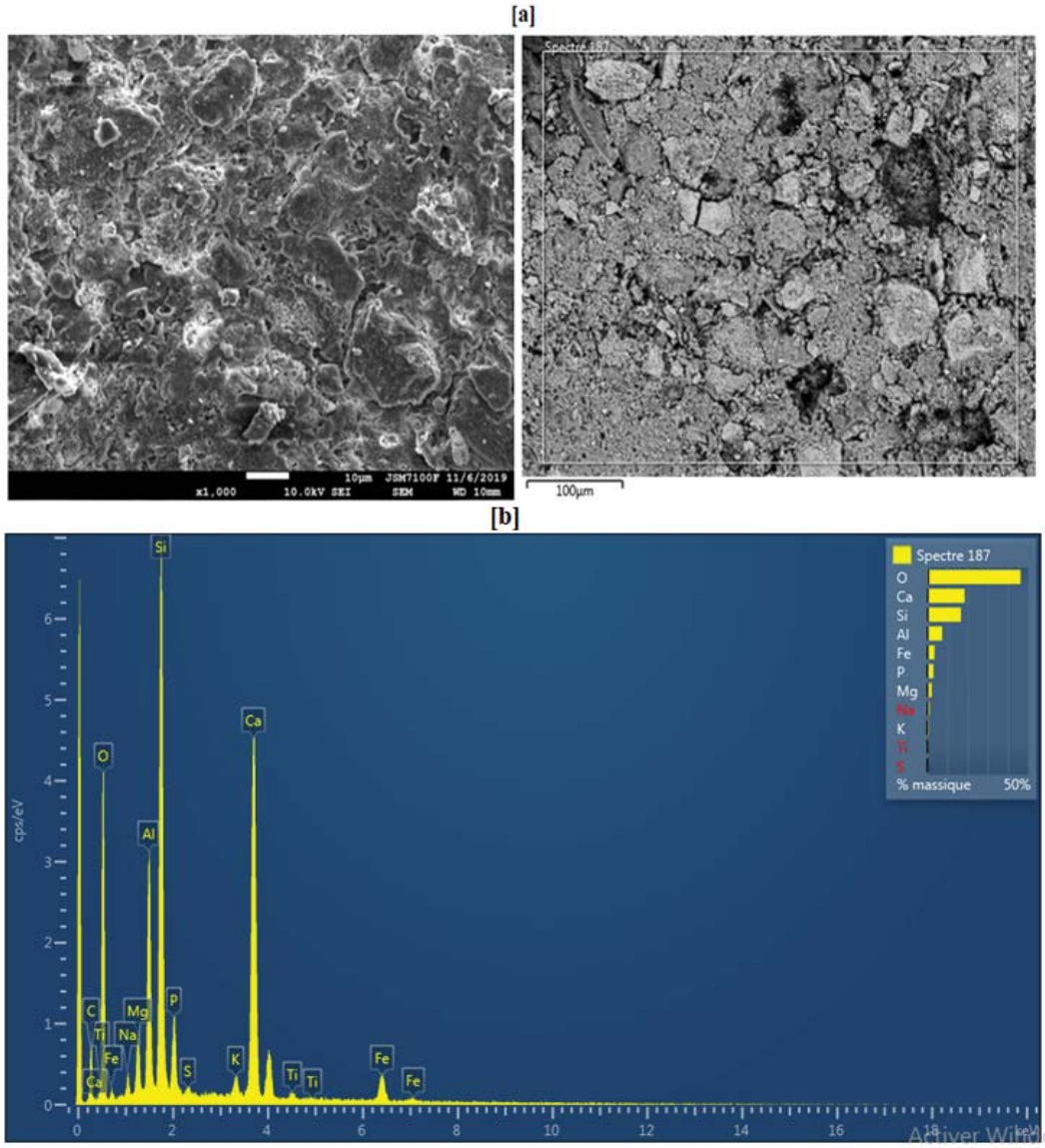

Fig. 7. (a) SEM morphology of the sintered substrate at 1,050°C and (b) EDX analysis of the sintered substrate at 1,050°C.

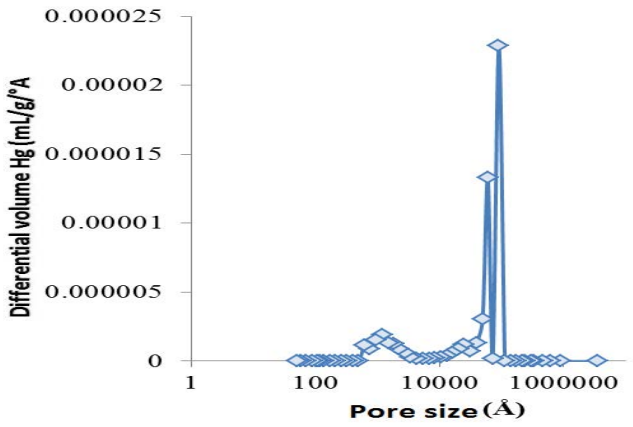

Fig. 8. Variation of porosity for the sintered ceramic support at 1,050°C.

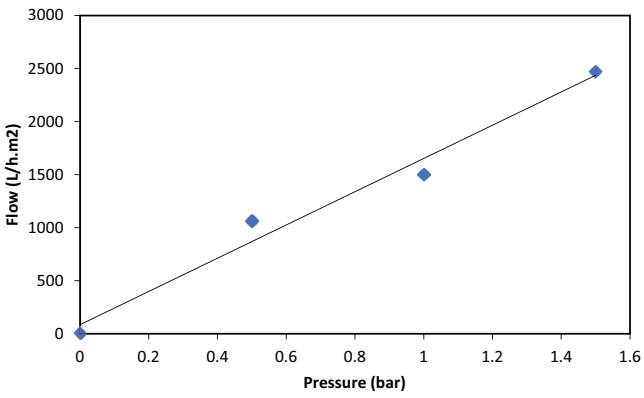

Fig. 9. Evolution of the flow (L/h·m²) of the microfiltration membrane according to the pressure (bar).

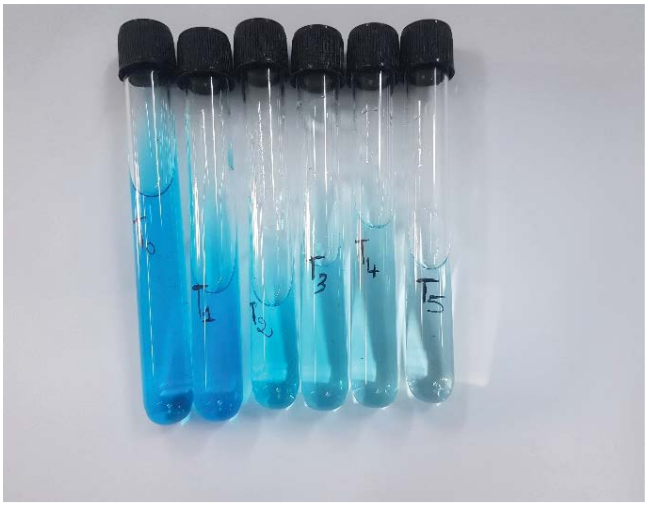

Fig. 10. Representative figure of the photocatalytic effect on the TiO_2 microfiltration membrane.

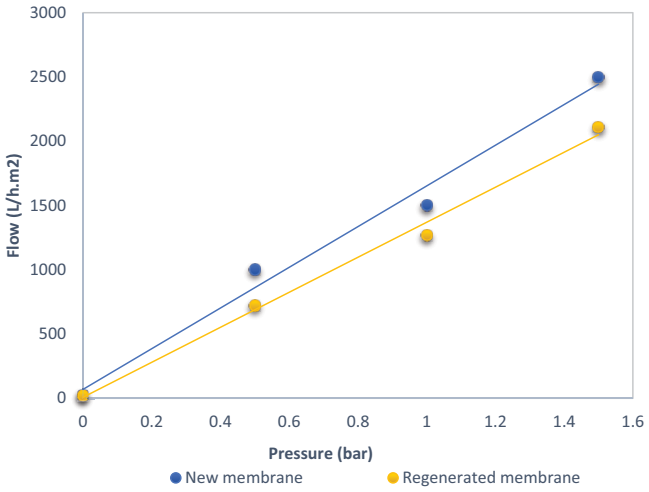

Fig. 11. Determination of water permeability for new and regenerated microfiltration membrane.

Subsequently, the ceramic was mounted on the filtration driver and the solution was poured on the membrane at a concentration of 100 mg/L.

As an initial step, the stability of the ceramic from a photocatalytic point of view was searched for. From this perspective, the membrane was put in the filtration pilot facing the solar radiation so as to achieve photocatalysis and degradation of the color. The basic objective underling this step was to observe the effect of TiO_2 layer on the degradation of turquoise blue. The stabilization time was around 60 min. In a second step, the solution was left to stabilize for 15 min. Next, the filtration device and the chronometer started to count the time that the test piece took to fill up with 10 mL. This procedure was repeated several times until the entire color degradation of the solution was obtained. Results of the filtration with photocatalysis revealed that the blue color was completely eliminated. The color was determined using 665 nm spectrophotometry.

The dye removal rate was 97.41%, which proves the high performance of this protocol (photocatalysis + filtration) for dye degradation (Fig. 10).

6. Membrane regeneration

The reusability of the membrane was also investigated so as to validate its application in industrial wastewater treatment. Therefore, after each experiment, the membrane should be regenerated by a wash cycle following the protocol of passing an aqueous NaOH solution (2%) at 80°C for 20 min, followed by a deionized water rinse until the pH is new. Then, it was washed with aqueous nitric acid (2%) at 60°C for 20 min, followed by a rinse with deionized water until the pH is neutral [14]. The efficiency of regeneration is determined by measuring the water permeability of the membrane. This permeability should be very similar to that obtained with freshly prepared membranes. Fig. 11 displays a quasi-complete regeneration of the membrane. This result suggests that membrane performance is maintained for a long time.

7. Conclusion

In the current research work, a new TiO_2 MF ceramic membrane developed on a substrate produced from Tunisian natural clay and phosphate was assessed for the treatment of wastewater from the textile industry. It was tested experimentally using various charges. The main finding of this study yields the following concluding remarks:

- the permeability of the support is roughly 2,526 L/h·m²·bar.
- the mechanical strength of the supports reaches its maximum at the sintering temperature of 1,100°C (σ = 30.87 MPa).
- SEM analysis revealed a porous structure for the ceramic. The cross-sectional view of the SEM image as well as the linear EDX analysis of the image displayed a regular membrane thickness of 100 µm. There is also a smoothing of the grains on the surface giving rise to a low roughness, which may entail the deposition of a layer.
- the substrates used at the optimum sintering temperature of 1,050°C have an average pore diameter of 10.36 µm and an average porosity of 41.66%.
- the permeability of the filter layer is nearly 2,526 L/h·m²·bar.
- the application of the membrane to the treatment of textile effluents by photocatalysis demonstrates a good degradation of dyes with a removal rate of 97.41%.

These results can be regarded as promising, worthwhile, and valuable as this new ceramic membrane can facilitate the treatment and management of industrial wastewater.

References

[1] T. Akimoto, H. Hasegawa, H. Ishihata, K. Kudo, D. Ishida, T. Kaneko, C. Kanno, M. Endo, M. Yamazaki, T. Kitabatake, S. Yaginuma, H. Honma, H. Ishihata, Alveolar bone augmentation with a newly designed microperforated pure titanium membrane: a clinical case series, J. Oral Maxillofac. Surg. Med. Pathol., 34 (2022) 389–394.

[2] H. Tong, C. Yang, Y. Lv, L. Wang, K. Chen, X. Zhou, Fabrication of tubular porous titanium membrane electrode and application in electrochemical membrane reactor for treatment of wastewater, J. Ind. Eng. Chem., 96 (2021) 269–276.
[3] Y. Gao, G. Xu, P. Zhao, L. Liu, E. Zhang, One step co-sintering synthesis of gradient ceramic microfiltration membrane with mullite/alumina whisker bi-layer for high permeability oil-in-water emulsion treatment, Sep. Purif. Technol., 305 (2023) 122400, doi: 10.1016/j.seppur.2022.122400.
[4] E. Eray, V.M. Candelario, V. Boffa, H. Safafar, D.N. Østedgaard-Munck, N. Zahrtmann, H. Kadrispahic, M.K. Jørgensen, A roadmap for the development and applications of silicon carbide membranes for liquid filtration: recent advancements, challenges, and perspectives, Chem. Eng. J., 414 (2021) 128826, doi: 10.1016/j.cej.2021.128826.
[5] Y. Wang, C. Yuan, K. Zhou, Q. Gu, W. Jing, Z. Zhong, W. Xing, Construction of Janus silicon carbide membranes with asymmetric wettability for enhanced antifouling in water-in-oil emulsification process, J. Membr. Sci., 671 (2023) 121389, doi: 10.1016/j.memsci.2023.121389.
[6] J. Zhang, N. Chen, M. Li, C. Feng, Synthesis and environmental application of zirconium–chitosan/graphene oxide membrane, J. Taiwan Inst. Chem. Eng., 77 (2017) 106–112.
[7] V.S. Silva, B. Ruffmann, H. Silva, V.B. Silva, A. Mendes, L.M. Madeira, S. Nunes, Zirconium oxide hybrid membranes for direct methanol fuel cells—evaluation of transport properties, J. Membr. Sci., 284 (2006) 137–144.
[8] B.D. Marshall, J.W. Allen, R.P. Lively, A model for the separation of complex liquid mixtures with glassy polymer membranes: a thermodynamic perspective, J. Membr. Sci., 647 (2022) 120316, doi: 10.1016/j.memsci.2022.120316.
[9] M.M. Merrick, R. Sujanani, B.D. Freeman, Glassy polymers: historical findings, membrane applications, and unresolved questions regarding physical aging, Polymer, 211 (2020) 123176, doi: 10.1016/j.polymer.2020.123176.
[10] J. Mo, X. Li, Z. Yang, Dissecting the structure-property relationship of ceramic membrane with asymmetric multilayer structures for maximizing permselectivity, Water Res., 220 (2022) 118658, doi: 10.1016/j.watres.2022.118658.
[11] T. Chen, Y. Xu, Y. Zhang, Y. Gong, Y. Zhang, J.Y.S. Lin, Double-layer ceramic-carbonate hollow fiber membrane with superior mechanical strength for CO_2 separation, J. Membr. Sci., 658 (2022) 120701, doi: 10.1016/j.memsci.2022.120701.
[12] Y. Liu, X. Zhang, W. Zhang, N. Wang, M. Jia, Z. Qin, H. Guo, Polyamide nanofiltration membrane with MoS_2 interlayer on tubular ceramic substrate for desalination, Desalination, 549 (2023) 116332, doi: 10.1016/j.desal.2022.116332.
[13] W. Aloulou, W. Hamza, H. Aloulou, A. Oun, S. Khemakhem, A. Jada, S. Chakraborty, S. Curcio, R. Ben Amar, Developing of titania-smectite nanocomposites UF membrane over zeolite based ceramic support, Appl. Clay Sci., 155 (2018) 20–29.
[14] Y. Yang, N. Ma, X. Wu, X. Lu, Z. Yin, H. Zhang, Z. Wang, Induction of zeolite membrane formation by implanting zeolite crystals into the precursor of ceramic supports, J. Membr. Sci., 635 (2021) 119452, doi: 10.1016/j.memsci.2021.119452.
[15] N. Kyriakou, M.-A. Pizzoccaro, A. Nijmeijer, M. Luiten-Olieman, L. Winnubst, Hydrolytic stability of PEG-grafted γ-alumina membranes: alkoxysilane vs phosphonic acid linking groups, Microporous Mesoporous Mater., 307 (2020) 110516, doi: 10.1016/j.micromeso.2020.110516.
[16] X. Chen, Y. Lin, Y. Lu, M. Qiu, W. Jing, Y. Fan, A facile nanoparticle doping sol–gel method for the fabrication of defect-free nanoporous ceramic membranes, Colloids Interface Sci. Commun., 5 (2015) 12–15.
[17] G. Xomeritakis, Y.S. Lin, Fabrication of a thin palladium membrane supported in a porous ceramic substrate by chemical vapor deposition, J. Membr. Sci., 120 (1996) 261–272.
[18] K. Ramesh, C. Sankha, P. Parimal, Membrane-integrated physico-chemical treatment of coke-oven wastewater: transport modelling and economic evaluation, Environ. Sci. Pollut. Res., 22 (2015) 6010–6023.
[19] S.-H. Lee, K.-C. Chung, M.-C. Shin, J.-I. Dong, H.-S. Lee, K.H. Auh, Preparation of ceramic membrane and application to the crossflow microfiltration of soluble waste oil, Mater. Lett., 52 (2002) 66–71.
[20] L. Cot, A. Ayral, J. Durand, C. Guizard, N. Hovnanian, A. Julbe, A. Larbot, Inorganic membranes and solid state sciences, Solid State Sci., 2 (2000) 313–334.
[21] K.L. Yeung, J.M. Sebastian, A. Varma, Mesoporous alumina membranes: synthesis, characterization, thermal stability and nonuniform distribution of catalyst, J. Membr. Sci., 131 (1997) 9–28.
[22] A.L. Ahmad, N.A. Abdullah Sani, S.H. Sharif Zein, Synthesis of a TiO_2 ceramic membrane containing $SrCo_{0.8}Fe_{0.2}O_3$ by the sol–gel method with a wet impregnation process for O_2 and N_2 permeation, Ceram. Int., 37 (2011) 2981–2989.
[23] N. Abidi, J. Duplay, A. Elmchaouri, A. Jada, M. Trabelsi-Ayadi, Textile dye adsorption onto raw clay: influence of clay surface properties and dyeing additives, J. Colloid Sci. Biotechnol., 3 (2014) 98–110.
[24] F. Bouzerara, R. Harabi, S. Achour, A. Larbot, Porous ceramic supports for membranes prepared from kaolin and doloma mixtures, J. Eur. Ceram. Soc., 26 (2006) 1663–1671.
[25] M. Khemakhem, S. Khemakhem, S. Ayedi, R. Ben Amar, Study of ceramic ultrafiltration membrane support based on phosphate industry subproduct: Application for the cuttlefish conditioning effluents treatment, Ceram. Int., 37 (2011) 3617–3625.
[26] B. Achiou, H. Elomari, M. Ouammou, A. Albizane, J. Bennazha, S. Alami Younssi, I.E. El Amrani, A. Aaddane, Elaboration and characterization of flat ceramic microfiltration membrane made from natural Moroccan pozzolan (Central Middle Atlas), J. Mater. Environ. Sci., 7 (2016) 196–204.
[27] B. Achiou, H. Elomari, A. Bouazizi, A. Karim, M. Ouammou, A. Albizane, J. Bennazha, S. Alami Younssi, I.E. El Amrani, Manufacturing of tubular ceramic microfiltration membrane based on natural pozzolan for pretreatment of seawater desalination, Desalination, 419 (2017) 181–187.
[28] A. Majouli, S. Tahiri, S. Alami Younssi, H. Loukili, A. Albizane, Elaboration of new tubular ceramic membrane from local Moroccan Perlite for microfiltration process. Application to treatment of industrial wastewaters, Ceram. Int., 38 (2012) 4295–4303.
[29] B. Das, B. Chakrabarty, P. Barkakati, Preparation and characterization of novel ceramic membranes for micro-filtration applications, Ceram. Int., 42 (2016) 14326–14333.
[30] S.M. Doke, G.D. Yadav, Synthesis of novel titania membrane support via combustion synthesis route and its application in decolorization of aqueous effluent using microfiltration, Clean Technol. Environ. Policy, 18 (2016) 139–149.
[31] Q. Gu, M. Kotobuki, C.H. Kirk, M. He, G.J.H. Lim, T.C.A. Ng, L. Zhang, H.Y. Ng, J. Wang, Overcoming the trade-off between water permeation and mechanical strength of ceramic membrane supports by interfacial engineering, ACS Appl. Mater. Interfaces, 13 (2021) 29199–29211.
[32] B.K. Nandi, R. Uppaluri, M.K. Purkait, Preparation and characterization of low cost ceramic membranes for micro-filtration applications, Appl. Clay Sci., 42 (2008) 102–110.
[33] S. Khemakhem, A. Larbot, R. Ben Amar, New ceramic microfiltration membranes from Tunisian natural materials: application for the cuttlefish effluents treatment, Ceram. Int., 35 (2009) 55–61.
[34] G.C. Sahoo, R. Halder, I. Jedidi, A. Oun, H. Nasri, P. Roy-choudhurry, S. Majumdar, S. Bandyopadhyay, R. Ben Amar, Preparation and characterization of microfiltration apatite membrane over low cost clay-alumina support for decolorization of dye solution, Desal. Water Treat., 57 (2016) 27700–27709.
[35] R. Das, S. Sarkar, S. Chakraborty, H. Choi, C. Bhattacharjee, Remediation of antiseptic components in wastewater by photocatalysis using TiO_2 nanoparticles, Ind. Eng. Chem. Res., 53 (2014) 3012–3020.
[36] P. Bhattacharya, S. Ghosh, S. Majumdar, S.N. Roy, S. Bandyo-padhyay, Ceramic membrane based microfiltration for treatment of highly contaminated tannery wastewater, Environ. Eng. Manage. J., 14 (2015) 2139–2148.

[37] N. El Baraka, N. Saffaj, R. Mamouni, A. Laknifli, S. Alami Younssi, A. Albizane, M. El Haddad, Elaboration of a new flat membrane support from Moroccan clay, Desal. Water Treat., 52 (2014) 1357–1361.
[38] G. Wu, Y. Wang, S. Zhu, J. Wang, Preparation of ultrafine calcium carbonate particles with micropore dispersion method, Powder Technol., 172 (2007) 82–88.
[39] K. Kandori, N. Horigami, A. Yasukawa, T. Ishikawa, Texture and formation mechanism of fibrous calcium hydroxyapatite particles prepared by decomposition of calcium–EDTA chelates, J. Am. Ceram. Soc., 80 (2005) 1157–1164.
[40] B.A. Sava, T. Vişan, Raman and FTIR studies of some sol-gel based glasses in the ZnO-TiO_2-SiO_2 system, U.P.B. Sci. Bull. Ser. B, 69 (2007) 11–24.
[41] M. Khemakhem, S. Khemakhem, R. Ben Amar, Emulsion separation using hydrophobic grafted ceramic membranes by air gap membrane distillation process, Colloids Surf., A, 436 (2013) 402–407.
[42] M.M. Mohamed, F.I. Zidan, M.H. Fodail, Synthesis of ZSM-5 zeolite of improved bulk and surface properties via mixed templates, J. Mater. Sci., 42 (2007) 4066–4075.
[43] M. Mouiya, A. Abourriche, A. Benhammou, Y. El Hafiane, Y. Abouliatim, L. Nibou, M. Oumam, H. Hannache, A. Smith, Porous ceramic from Moroccan natural phosphate and raw clay for microfiltration applications, Desal. Water Treat., 83 (2017) 277–280.
[44] Z. Anari, A. Sengupta, K. Sardari, S. Ranil Wickramasinghe, Surface modification of PVDF membranes for treating produced waters by direct contact membrane distillation, Sep. Purif. Technol., 224 (2019) 388–396.
[45] R.L. Frost, S.J. Palmer, Y. Xi, J. Čejka, J. Sejkora, J. Plášil, Raman spectroscopic study of the hydroxy-phosphate mineral plumbogummite $PbAl_3(PO_4)_2(OH,H_2O)_6$, Spectrochim. Acta, Part A, 103 (2013) 431–434.
[46] S.J. Joris, C.H. Amberg, Nature of deficiency in nonstoichiometric hydroxyapatites. II. Spectroscopic studies of calcium and strontium hydroxyapatites, J. Phys. Chem., 75 (1971) 3172–3178.